

Design and Simulation of 50 nm Vertical Double-Gate MOSFET (VDGM)

Ismail Saad and Razali Ismail

Faculty of Electrical Engineering, Universiti Teknologi Malaysia, 81310, Skudai, Johor

e-mail: ismail_s@ums.edu.my, razali@fke.utm.my

Abstract The paper demonstrate the design and simulation study of 2D Vertical Double-Gate MOSFET (VDGM) with an excellent short channel effect (SCE) characteristics. With the gate length of 50nm, body doping of $3.5 \times 10^{18} \text{ cm}^{-3}$ and oxide thickness, $T_{\text{OX}} = 2.5\text{nm}$, a good drive current I_{ON} of $7 \mu\text{A}/\mu\text{m}$ and a low off-state leakage current I_{OFF} of $2 \text{ pA}/\mu\text{m}$ was explicitly shown. Besides that, the subthreshold characteristics also highlighted a reasonably well-controlled SCE with subthreshold swing $\text{Sub}V_{\text{T}} = 89 \text{ mV/decade}$ and threshold voltage $V_{\text{T}} = 0.56\text{V}$. The analysis of body doping effects for SCE optimization and drive current trade-off was also done for an overall investigation and limit of the VDGM.

I. INTRODUCTION

With the advantages of controlled gate length by a relax photolithographic process, high drives current per unit silicon area and decoupled channel length from packing density, Vertical double-gate (VDGM) and/or surround gate (VSGM) MOSFET become prominent candidate to extend CMOS technology to and beyond the 45nm as depicted by International Technology Roadmap for Semiconductor, ITRS [1]. In contrast, the planar double-gate (DG) has also been intensively in research. The focus is on new structure such as Self-aligned FinFet structure [2, 3, 4], Silicon On Nothing (SON) [5], PAGODA concept [6] and Bonded double-gate [7]. However, this planar device requires advanced processes and precise definition of channel length that make it less acceptable compared with Vertical channel types. Generally, the vertical type MOSFET can be categorized according to channel definition fabrication method. It can be ion implanted process [8-15], epitaxially grown [16-19], and retarded etching [20] on the sidewalls of Silicon pillars. In this paper the structure of a Vertical replacement gate transistor [19], in which the source/drain

electrodes are defined by solid state diffusion after channel epitaxial growth is been analyzed with a double-gate configuration. The VDGM device was design and simulated using 2D commercial device simulation (ATLAS) software [21]. The utilization of such process and device simulation for an investigation and detail analysis of new device structure has been raised sharply. Such methods are employed in [22-24]. Using such standard, we demonstrate the design of 2 Dimensional vertical double-gates MOSFET (VDGM) with an excellent short channel effect (SCE) feature. With the gate length of 50nm, body doping of $3.5 \times 10^{18} \text{ cm}^{-3}$ and oxide thickness, $T_{\text{OX}} = 2.5\text{nm}$, a good drive current I_{ON} of $7 \mu\text{A}/\mu\text{m}$ and a low off-state leakage current I_{OFF} of $2 \text{ pA}/\mu\text{m}$ was obtained. In addition, the subthreshold characteristics also highlighted a reasonably well-controlled short channel effects (SCE) with subthreshold swing $\text{Sub}V_{\text{T}} = 89 \text{ mV/decade}$ and threshold voltage $V_{\text{T}} = 0.56\text{V}$. An effect of lowering the body doping for getting an acceptable I_{OFF} and V_{T} as it will increase the surface mobility and drive current was also done. However, an optimization is needed as a high body doping was essential for controlling SCE. The trade-off between controlling SCE with an optimize level of body doping was done explicitly in this paper.

II. MODELING PROCEDURE

The simulated VDGM structure is shown in figure 1a and 1b with the double gate region (in contact), drain and source electrode, channel length L_{g} , silicon oxide T_{ox} , silicon body and the respective dimensions of the device is explicitly shown. The process start with a mesh or grid definition in which the critical area such as L_{g} and T_{ox} were given a finer mesh compare to other regions. Subsequently, the coordinates of source, drain, body, left and right gate, gate oxide and separation oxide region were defined. The electrode region of drain, source and double gate area were also formed for the contacts to be

used in device characterization process later. Notice that an electrode line is visible in figure 1a for making sure that the left and right gate was in contacts. Later, a uniform doping profile is assumed and applied to drain (n-type), source (n-type), double gate (n-type) and body (p-type) of the device with the concentration of $1 \times 10^{20} \text{ cm}^{-3}$, $1 \times 10^{20} \text{ cm}^{-3}$, $1 \times 10^{21} \text{ cm}^{-3}$ and $3.5 \times 10^{18} \text{ cm}^{-3}$ respectively. The channel body doping may be varied for an analysis on its effects in device performance.

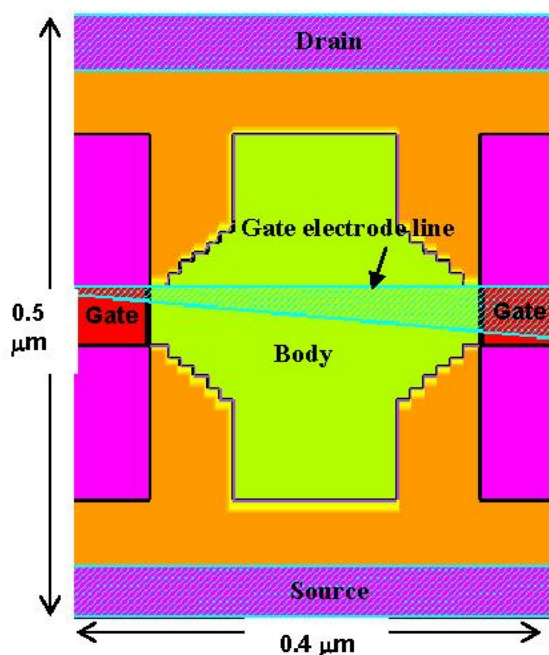


Fig.1a. Vertical Double-Gate MOSFET (VDGM) structure showing double gate, source, drain, and body

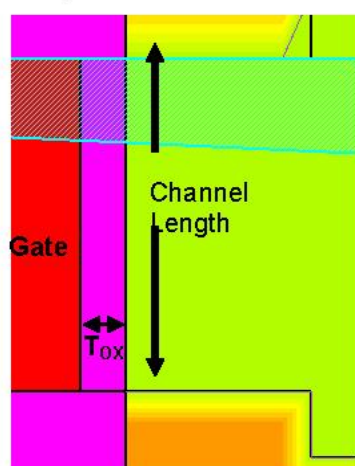


Fig.1b. Vertical Double-Gate MOSFET (VDGM) structure showing channel length and oxide thickness

The inversion layer mobility model from Lombardi [21] was employed for its dependency

on the transverse field (i.e field in the direction perpendicular E_{\perp} to the Si/SiO₂ interface of the MOSFET) and through velocity saturation at high longitudinal field (i.e field in the direction from source-to drain parallel E_{\parallel} to the Si/SiO₂ interface) combined with SRH (Shockley-Read-Hall Recombination) with fixed carrier lifetimes models [21]. This recombination model was selected since its take into account the phonon transitions effect due to the presence of a trap (or defect) within the forbidden gap of the semiconductor. An interface fixed oxide charge of 3×10^{10} is assumed with the used of n-type Polysilicon gate contact for the device. The Drift-Diffusion transport [21] model with simplified Boltzmann carrier statistics [21] is employed for numerical computation of the design device.

III. ELECTRICAL CHARACTERIZATION

The combination of Gummel and Newton numerical methods [21] was employed for a better initial guess in solving quantities for obtaining a convergence of the device structure. Figure 2 shows the current-voltage ($I_{GS} - V_{GS}$) characteristics for VDGM device with channel length $L_g = 50 \text{ nm}$, oxide thickness $T_{OX} = 2.5 \text{ nm}$ and body channel doping $N_A = 3.5 \times 10^{18} \text{ cm}^{-3}$. By using a linear extrapolation of transconductance $g_m(V_{GS})$ to zero [25] a 0.56 V threshold voltage V_T was obtained for both $V_{DS} = 1.2 \text{ V}$ and 0.1 V in the linear operated region.

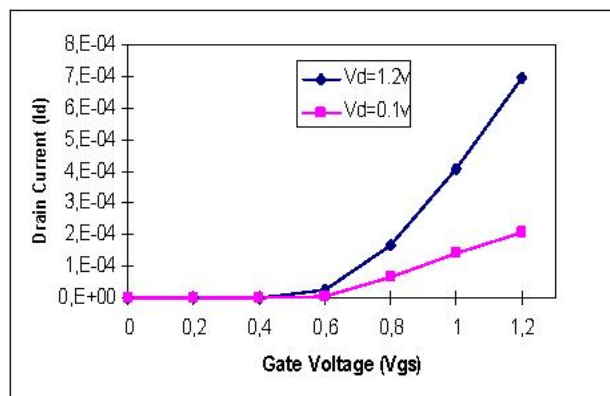


Fig. 2. Current-Voltage characteristic of VDGM with $L_g = 50 \text{ nm}$, $T_{OX} = 2.5 \text{ nm}$, $N_A = 3.5 \times 10^{18} \text{ cm}^{-3}$ and $V_T = 0.56 \text{ V}$ taken at $V_{DS} = 0.1 \text{ V}$ and 1.2 V

A low $V_T = 0.56 \text{ V}$ extracted for this device yield that a low power consumption of the MOSFET device is maintained and is comparably better

with a planar MOSFET for deep sub-micron device [13, 16, 17]. However, this V_T is considerably high for 1.2V intended circuit operation due to a high channel doping N_A that reduces the surface mobility and degrade the drive current I_{ON} . However, high doping is necessary for controlling the SCE. An output characteristic $I_{DS}-V_{DS}$ is shown in figure 3, that explicitly illustrate a moderately low drain current due to a high doping.

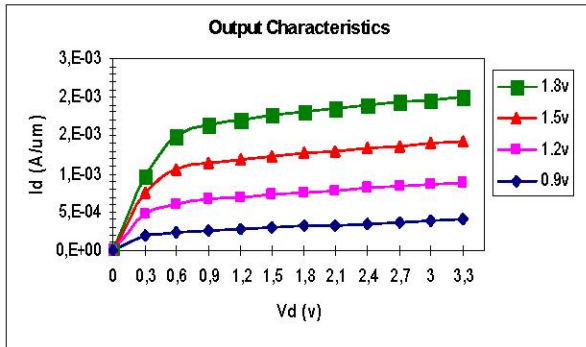


Fig. 3. Output characteristic of VDGM with $L_g=50\text{nm}$, $T_{OX}=2.5\text{nm}$, $N_A=3.5 \times 10^{18} \text{ cm}^{-3}$ and $V_T=0.56\text{V}$ for $V_{GS}=0.9, 1.2, 1.5$ and 1.8V .

Figure 4 shows a good off-state leakage current I_{OFF} of 2 pA/μm and drive current I_{ON} of 7 μA/μm due to high doping that control the off and on state of the device. Furthermore, reasonably well-controlled SCE with subthreshold swing $\text{Sub}V_T = 89 \text{ mV/decade}$ is also highlighted in figure 4.

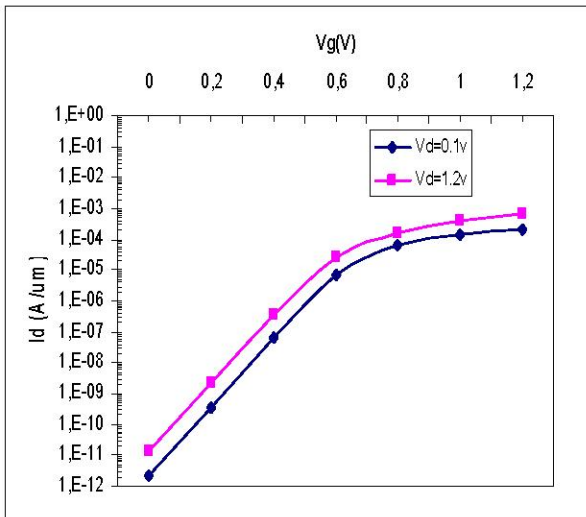


Fig. 4. Subthreshold characteristic of VDGM with $L_g=50\text{nm}$, $T_{OX}=2.5\text{nm}$, $N_A=3.5 \times 10^{18} \text{ cm}^{-3}$ and $I_{OFF}=2\text{pA}/\mu\text{m}$, $I_{ON}=7\mu\text{A}/\mu\text{m}$, $\text{Sub}V_T=89\text{mV/dec}$

Further analysis on the VDGM performance was done by comparing its capability to control SCE with single gate MOSFET. By applying the same mobility and recombination model with different channel length which is higher by a factor of 50 in single gate MOS, the resulted subthreshold characteristics is shown in figure 5.

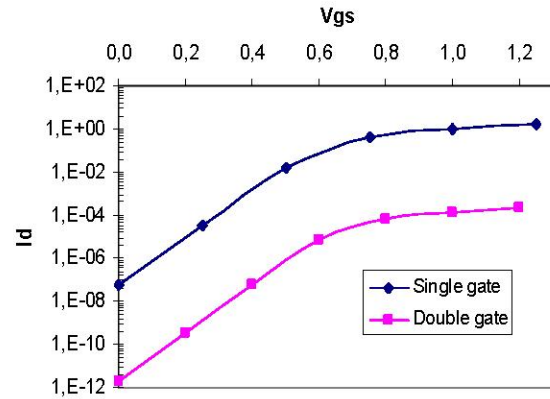


Fig. 5. Comparison of Subthreshold characteristic of VDGM with Single gate MOSFET (SGM). Low leakage current is exhibited in VDGM in pico range as with SGM.

As expected, the vertical double gate give a low off-state leakage current as compared to single gate MOSFET (SGM) and an acceptable OFF/ON ratio due to a better control of electrostatic potential in gate region for the vertical defined channel [8, 9, 10]. However, these was achieved due to a high body doping in VDGM which gave a good SCE control with a high threshold voltage due to a degradation in surface mobility as depicted in figure 2 and consequently reduced the drain current as shown in figure 3. Thus, the effect of body doping has to be analyzed for obtaining an acceptable V_T , I_{DS} and optimize control of SCE. This will be carried out in the next section.

V. DOPING EFFECT ANALYSIS

Three variant of body doping are used: low doped ($N_a = 1 \times 10^{18} \text{ cm}^{-3}$), moderately doped ($N_a = 2 \times 10^{18} \text{ cm}^{-3}$) and the high doped ($N_a = 3.5 \times 10^{18} \text{ cm}^{-3}$). In Figure 6 we can see that V_T is reduced as the doping level is decreased.

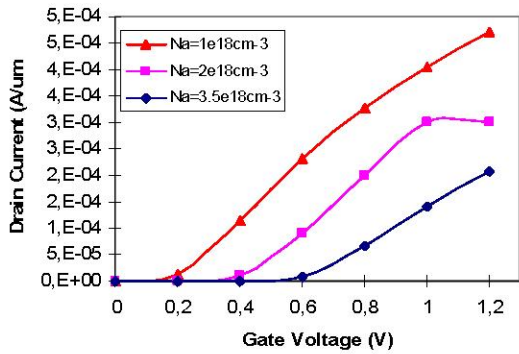


Fig.6. I_{GS} - V_{GS} characteristic of VDGM shows a decreased in V_T is observed with a lower doping level.

The V_T value decreases from 0.56V for high doped to 0.36V in moderate doped and to a lower value of 0.15V in low doped body. Further analysis is done, by comparing the subthreshold characteristics with different doping level as shown in figure 7.

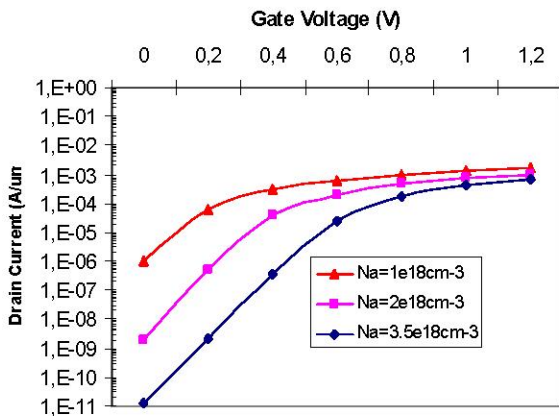


Fig.7. Subthreshold characteristic of VDGM showing an increased in leakage and drive current with a lower doping level.

As can be seen in figure 7, a decreased in doping will ultimately increased the leakage current from $2\text{pA}/\mu\text{m}$ to $7\text{nA}/\mu\text{m}$ and finally to a value of $80\mu\text{A}/\mu\text{m}$. However, the increased in drive current is almost unity with a value of $7\mu\text{A}/\mu\text{m}$ to $10\mu\text{A}/\mu\text{m}$ and $1\text{mA}/\mu\text{m}$ respectively. These effects arise due to the fact that at higher doping the surface mobility is decreased and a better gate electrostatic potential observed within the device which makes the leakage current controllable. However, as the doping level decreased, the carrier mobility is increased and consequently the leakage current will also rise sharply. On the other hand, since the channel is defined vertically with a double gate

configuration, a unity drive current is observed which also increased with a decreased in doping level. Due to a double gate arrangement the increased in drain current (I_{DS}) was observed as shown in figure 8 of the output characteristics.

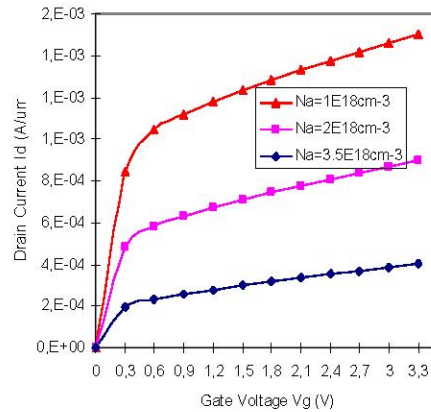


Fig.8. Output characteristic of VDGM shows an increased in Drain current with a lower doping level in a double-gate configuration.

Even though the drive current is high with lower doping level, a high leakage current is observed in figure 7, $I_{OFF} = 80\mu\text{A}/\mu\text{m}$ is highly unacceptable. These results are in conjunction with the value of subthreshold voltage obtained, which is 89 mV/decade for higher doped, 83 mV/decade in moderate doped and sharply increased to 110 mV/decade in lower doped device as depicted in figure 7. Thus, an optimize value of body doping is highly vital in order to have a high drive current while maintaining the acceptable leakage current and controlling the aggravated SCE. If one fails to control such parameters, the transistor designed will not succeed to work in a giga-scaled integrated circuit where the total standby power of the system is of paramount important.

VI. CONCLUSION

The design of a 50nm Vertical Double Gate MOSFET (VDGM) device based on the structure reported in [19] has been successfully done using commercial ATLAS TCAD tools. By employing the inversion layer mobility model from Lombardi combined with SRH (Shockley-Read-Hall Recombination) with fixed carrier lifetimes models with an interface fixed oxide charge of 3×10^{10} assumed and the used of n-type Polysilicon gate contact, a detailed investigation on the VDGM performance was done. With the gate length of 50nm, body doping of 3.5×10^{18}

cm^{-3} and oxide thickness, $T_{\text{OX}} = 2.5\text{nm}$, a good drive current I_{ON} of $7\ \mu\text{A}/\mu\text{m}$ and a low off-state leakage current I_{OFF} of $2\ \text{pA}/\mu\text{m}$ was obtained. In addition, the subthreshold characteristics also highlighted a reasonably well-controlled short channel effects (SCE) with subthreshold swing $\text{Sub}V_{\text{T}} = 89\ \text{mV}/\text{decade}$ and threshold voltage $V_{\text{T}} = 0.56\text{V}$. The effects of body doping N_{A} in obtaining a good drive current I_{ON} while maintaining an acceptable leakage current I_{OFF} , threshold voltage V_{T} and subthreshold voltage $\text{Sub}V_{\text{T}}$ for controlling the SCE was investigated. With a moderate body doping level $N_{\text{A}} = 2.0 \times 10^{18}\ \text{cm}^{-3}$, a threshold voltage $V_{\text{T}} = 0.36\text{V}$, leakage current $I_{\text{OFF}} = 7\ \text{nA}/\mu\text{m}$ and $\text{Sub}V_{\text{T}} = 83\ \text{mV}/\text{decade}$ and a good drive current $I_{\text{ON}} = 10\ \mu\text{A}/\mu\text{m}$ was successfully obtained and optimized for the simulated VDGGM device.

REFERENCES

- [1] *International Technology Roadmap for Semiconductor (ITRS) – Emerging Research Devices*. <http://public.itrs.net>, 2005
- [2] Xuejue Huang et., al. “Sub-50nm P-Channel FinFet”. IEEE Transactions on Electron Devices, vol.48, no.5, May 2001
- [3] Xuejue Huang et., al. “Sub 50nm FinFET : PMOS”. IEDM 1999
- [4] Bin Yu et., al. “FinFET Scaling to 10nm Gate Length”. IEDM 2002
- [5] S. Harrison et., al. “Highly Performant Double Gate MOSFET realized with SON process”. IEDM 2003
- [6] M. Vinet et., al. “Bonded Planar Double-Metal-Gate NMOS Transistors Down to 10 nm”. IEEE Transactions on Electron Devices, vol.26, no.5, May 2005
- [7] P.M. Solomon et., al. “Two Gates are Better than One”. IEEE Circuits & Devices Magazine, January 2003
- [8] Gili et., al. “Asymmetric Gate-Induced Drain Leakage and Body Leakage in Vertical MOSFETs With Reduced Parasitic Capacitance”. IEEE Transactions on Electron Devices, vol.53, no.5, May 2006
- [9] Enrico Gili et., al. “Single, Double and Surround gate vertical MOSFETs with reduced parasitic capacitance”. Solid-State Electronics 48 (2004) pg 511-519
- [10] V.D Kunz et., al. “Reduction of Parasitic Capacitance in Vertical MOSFETs by Spacer Local Oxidation”; IEEE Transactions on Electron Devices, VOL. 50, pp 1487-1493, June 2003
- [11] Enrico Gili, et., al. “Electrical Characteristics of Single, Double & Surround Gate Vertical MOSFETs with Reduced Overlap Capacitance”; ESSDERC 2003
- [12] V.D Kunz et., al. “CMOS-compatible vertical MOSFETs and logic gates with reduced parasitic capacitance”; ESSDERC 2004
- [13] D. Donaghy et., al. “Design of 50nm Vertical MOSFET Incorporating a Dielectric Pocket”. IEEE Transactions on Electron devices, vol.51, no.1, January 2004
- [14] Enrico Gili et., al. “A new approach to the fabrication of CMOS compatible vertical MOSFETs incorporating a dielectric pocket”. ULIS 2005
- [15] Thomas Schulz et., al. “Short-Channel Vertical Sidewall MOSFETs”. IEEE Transactions on Electron devices, vol.48, no.8, August 2001
- [16] S.K. Jayanarayanan et., al. “A Novel 50nm vertical MOSFET with a dielectric pocket”. Solid-State Electronics 50 (2006) pg 897-900.
- [17] Kiyoshi Mori et., al. “Sub-100-nm Vertical MOSFET with Threshold Voltage Adjustment”. IEEE Transactions on Electron devices, vol.49, no.1, January 2002.
- [18] Haitao Liu et., al. “An Ultrathin Vertical Channel MOSFET for Sub-100-nm Applications”. IEEE Transactions on Electron devices, vol.50, no.5, May 2003.
- [19] J.M.Hergenrother et., al. “The Vertical replacement (VRG) MOSFET: A 50nm vertical MOSFET with lithography-independent gate length”. IEDM Tech. Dig., 1999, pp. 75-78
- [20] Meishoku Masahara et., al. “Ultrathin Channel Vertical DG MOSFET Fabricated by Using Ion-Bombardment-Retarded Etching”. IEEE Transactions on Electron devices, vol.51, no.12, December 2004.
- [21] Silvaco International, “ATLAS user Manual DEVICE SIMULATION SOFTWARE”
- [22] Ali A. Orouji et., al. “Shielded Channel Double-Gate MOSFET: A Novel Device for Reliable Nanoscale CMOS Applications” IEEE Transactions On Device And Materials Reliability, Vol. 5, No. 3, September 2005
- [23] G.Venkateshwar Reddy et., al.”A New Dual-Material Double-Gate (DMDG) Nanoscale SOI MOSFET—Two-Dimensional Analytical Modeling and Simulation”. IEEE Transactions On Nanotechnology, Vol. 4, No. 2, March 2005
- [24] Ismail Saad et., al. “Simulation of a Novel Lateral Bipolar Transistor with an approximately 21 GHz f_{TMAX} on Thin Film SOP”. Proc. International Workshop on The Physics of Semiconductor Devices (IWPSD-2003), IIT Madras, India, December 2003
- [25] M.Tsuno et al, “Physically-based Threshold voltage determination for MOSFETs of all gate length,” IEEE Trans. Electron Devices, vol. 46, pp. 1429-1434, July 1999